Application of Direct Current Potential Drop for the J-integral vs. Crack Growth Resistance Curve Characterization

Xiang (Frank) Chen[1], Randy K. Nanstad[1], Mikhail A. Sokolov[1]

[1]Materials Science and Technology Division, Oak Ridge National Laboratory

Abstract

The direct current potential drop (DCPD) technique has been applied to derive the J-integral vs. crack growth resistance curve (J-R curve) for fracture toughness characterization of structural materials. The test matrix covered three materials including type 316LN stainless steels, Ni-based alloy 617, and one ferritic-martensitic steel, three specimen configurations including standard compact, single edge bending, and disk-shaped compact specimens, and temperatures ranging from 20°C to 650°C. When compared with baseline J-R curves derived from the ASTM normalization method, the original J-R curves from the DCPD technique yielded much smaller J_q values due to the influence of crack blunting, plastic deformation, etc. on potential drop. To counter these effects, a new procedure for adjusting DCPD J-R curves was proposed. After applying the new adjustment procedure, the average difference in J_q between the

DCPD technique and the normalization method was only 5.2% and the difference in tearing modulus was 7.4%. The promising result demonstrates the applicability of the DCPD technique for the J-R curve characterization especially in extreme environments, such as elevated temperatures, where the conventional elastic unloading compliance method faces considerable challenges.

Introduction

To improve thermal efficiency, next generation nuclear reactors aim at operating at more severe environment, such as elevated temperatures and higher stress levels, than current reactors. Therefore, characterization of mechanical properties of structural materials for next generation nuclear reactors in extreme environments becomes vitally important from both an engineering design and a safety management point of view [1]. Among different mechanical properties of materials, J-integral vs. crack growth resistance curve (J-R curve) is a useful tool for evaluating material structural integrity in the presence of pre-existing defects. To date, extensive efforts have been continuously devoted to the development of simplified and reliable methods for determining material J-R curves. A widely accepted practice for conducting J-R curve testing is ASTM standard E1820-13 [2], in which the elastic unloading compliance (EUC) method is recommended for online crack length measurement. However, the EUC method becomes impractical in elevated temperature testing due to material stress relaxation resulting in nonlinear unloading-reloading curves (shown in Fig. 1(a)) and enhanced friction interference between the specimen, pins and clevises which results in a back-up shape of the J-R curve (shown in Fig. 1(b)). In addition, the EUC method may underpredict the crack extension for standard disk-shaped compact (DC(T)) specimens which further limits its applications for the J-R curve determination in small specimens [3].

In order to address these issues associated with the J-R curve determination with the EUC method, ASTM E1820-13 Annex 15 [2] introduces the normalization method as an alternative J-R curve characterization method. The normalization method was initially developed by Herrera and Landes et al. [4, 5] and later studied by Joyce and Lee [6, 7]. In contrast to the EUC method, the normalization method does not rely on the compliance measurement for on-line crack size measurement. Instead, the normalization method solely needs a load-displacement record taken together with initial and final crack size measurements from the specimen fracture surface to derive the material J-R curve. Because of the elimination of the compliance measurement, the load-displacement curve in the normalization method does not need to have the unloading-reloading portion as in the EUC method, which significantly simplifies the test and reduces the test time. Despite these advantages, the normalization method requires that the final physical crack extension in a J-R curve test cannot exceed the lesser of 4mm or 15% of the initial uncracked ligament [2]. Since the real-time crack extension is not available in a J-R curve test using the normalization method, it can be a great challenge to fulfill the crack extension requirement in the normalization method.

In order to develop a J-R curve test method suitable for extreme testing conditions and with reliable online crack length measurement, the direct current potential drop (DCPD) technique is investigated in this study. As another alternative J-R curve test method [8-12], the DCPD technique combines advantages of both the EUC method and the normalization method. It does not require the unloading compliance measurement, so elevated temperature testing issues using the EUC method are not experienced in the DCPD technique. In addition, the DCPD technique provides experimental real-time crack size measurements in contrast to the normalization method. Fig. 2 illustrates the crack length measurement principle in the DCPD

technique. As a constant direct current passes through the specimen, the subsequent voltage generated across the uncracked ligament in the specimen is measured. Once a crack propagates in the specimen, less area is available for the passage of the current, resulting in increases of the effective electrical resistance and an increase in the potential across the sample. Thus, the potential drop measurement in DCPD can be used to derive the real-time crack size if the correlation between the potential drop and the crack size is known.

In this work, material fracture toughness based on the J-R curve was characterized by the DCPD technique and results were compared with J-R curves derived from the ASTM normalization method. The test matrix covered a wide range of materials, specimen configurations, and testing temperatures to evaluate the applicability of the DCPD technique in the J-R curve characterization.

Experimental

Materials and Specimens

Three different materials, covering a broad category of metallic materials including type 316LN stainless steel (MatA), Ni-based alloy 617 (MatB), and one ferritic-martensitic steel (MatC), were selected in J-R curve testing.

Specimen configurations used in J-R curve testing include 0.5T standard compact (C(T)), 5x10mm and 10x10mm single edge bending (SE(B)), and 0.18T DC(T) specimens. The detailed specimen designs are shown in Fig. 3. Each specimen was fatigue pre-cracked until the initial crack length equaled 50% of the specimen width and then side-grooved to remove 10% of specimen thickness from each side of the specimen.

Test Conditions and Experimental Setup

The test matrix is summarized in Table 1. All tests were performed with a quasi-static loading rate such that the rate of increase of the stress intensity factor (dK/dt) during the initial elastic portion was 2 MPa√m/s. Test temperatures cover a wide range from 20°C to 650°C, representing conventional room temperature and elevated temperature J-R curve tests. For each test, load-displacement data and DCPD signals were acquired from the same specimen so that comparison of J-R curve results between the DCPD technique and the normalization method is made on the same specimen to avoid any influence due to specimen to specimen variations.

The experimental setup for performing J-R curve testing has been described previously [3, 13]. In summary, servo-hydraulic test frames were employed for loading specimens. For SE(B) and DC(T) specimens, the load-line displacement was measured, whereas, for C(T) specimens, crack mouth opening displacement (CMOD) on the specimen front face was measured[1]. For the DCPD data acquisition, current probes and potential probes were spot welded to each specimen configuration as shown in Fig. 3. The current probes were spot welded at one half of the specimen width and thickness location. The potential probes were spot welded diagonally across the starter notch to average measurements from non-uniform crack fronts if there are any [16].

Results and Discussion

The normalization method, described in more details in ref. [2, 13], is applied in this study to determine the baseline J-R curves. Then results are compared with J-R curves derived from the DCPD technique to evaluation the applicability of the DCPD technique in the J-R curve characterization.

J-R Curve Determination by the DCPD Technique

[1] The front face CMOD measurements for C(T) specimens were converted to load-line displacements by multiplying by a factor of 0.73 in following J-R curve analyses [14,15].

The DCPD technique derives experimental real-time crack sizes based on the potential drop measurement across an area in the specimen. A number of constitutive equations are available for converting the potential drop measurement into the crack size in the DCPD technique. Among those constitutive equations, Johnson's equation [17, 18] has been widely used and is given by:

$$a = \frac{2W}{\pi}\cos^{-1}\frac{\cosh(\pi y/2W)}{\cosh\{(U/U_0)\cosh^{-1}[\cosh(\pi y/2W)/\cos(\pi a_0/2W)]\}} \quad (1)$$

where a is the crack length corresponding to potential drop U, y is one half of the potential gage span (i.e. 4.445 mm for C(T), 2.5 mm for SE(B), and 1.27 mm for DC(T) per Fig. 3), W is the specimen width, and a_0 and U_0 are the initial crack length and the initial potential drop measurement, respectively.

Once the crack lengths in a J-R curve test become available, J-integral can be calculated by:

$$J_i = \frac{K_i^2(1-\nu^2)}{E} + J_{pli} \quad (2)$$

where K_i is the stress intensity at the i-th data point, ν is Poisson's ratio, E is Young's modulus of the material, and J_{pli} is the plastic component of J_i at the i-th data point. The equations for calculating K_i for C(T), SE(B), and DC(T) specimens respectively, are:

$$K_i = \frac{P_i}{(BB_N W)^{1/2}} \times \frac{(2+\frac{a_i}{W})[0.886+4.64(\frac{a_i}{W})-13.32(\frac{a_i}{W})^2+14.72(\frac{a_i}{W})^3-5.6(\frac{a_i}{W})^4]}{(1-\frac{a_i}{W})^{3/2}} \quad (3a)$$

$$K_i = \frac{P_i S}{(BB_N)^{1/2} W^{3/2}} \times \frac{3(\frac{a_i}{W})^{1/2}[1.99-(\frac{a_i}{W})(1-\frac{a_i}{W})(2.15-3.93(\frac{a_i}{W})+2.7(\frac{a_i}{W})^2)]}{2(1+2\frac{a_i}{W})(1-\frac{a_i}{W})^{3/2}} \quad (3b)$$

$$K_i = \frac{P_i}{(BB_N W)^{1/2}} \times \frac{(2+\frac{a_i}{W})[0.76+4.8(\frac{a_i}{W})-11.58(\frac{a_i}{W})^2+11.43(\frac{a_i}{W})^3-4.08(\frac{a_i}{W})^4]}{(1+\frac{a_i}{W})^{3/2}} \quad (3c)$$

where P_i is the load at the i-th data point, B is the specimen thickness, B_N is the specimen net thickness, a_i is the crack size at the i-th data point, and S is the specimen span dimension in SE(B) specimens. The equation for calculating J_{pli} is given by:

$$J_{pli} = [J_{pli-1} + \frac{\eta_{pli-1}}{b_{i-1}} \frac{A_{pli} - A_{pli-1}}{B_N}][1 - \gamma_{pli-1} \frac{a_i - a_{i-1}}{b_{i-1}}] \quad (4)$$

where J_{pli-1} is the plastic part of J-integral for the (i-1)-th data point and assuming J_{pl0} equals to zero (initial plastic component of J-integral is zero), b_{i-1} is the uncracked ligament for the (i-1)-th data point and equals to W-a_{i-1}, η_{pli-1} is a dimensionless parameter that relates plastic work done on a specimen to crack growth resistance defined in terms of deformation theory J-integral [19] and equals 1.9 for SE(B) specimens and 2.0+0.522b_{i-1}/W for C(T) and DC(T) specimens, and γ_{i-1} is a function to correct the J-integral evaluated by η_{pli-1} parameter in the crack growth situation [20] and equals 0.9 for SE(B) specimens and 1.0+0.76b_{i-1}/W for C(T) and DC(T) specimens. The quantity A_{pli}-A_{pli-1} is the increment of plastic area under the load verse plastic load-line displacement record between lines of constant plastic displacement v_{pli} and v_{pli-1} and can be calculated from the following equation:

$$A_{pli} - A_{pli-1} = \frac{(P_i + P_{i-1})(v_{pli} - v_{pli-1})}{2} \quad (5)$$

where v_{pli} is the plastic part of the i-th load-line displacement data point and is given by:

$$v_{pli} = v_i - P_i C_{LLi} \quad (6)$$

where v_i is the load-line displacement at the i-th data point and C_{LLi} is the equivalent compliance corresponding to a_i and for C(T), SE(B), and DC(T) specimens. C_{LLi} is calculated as:

$$C_{LLi} = \frac{1}{EB_e}\left(\frac{W+a_i}{W-a_i}\right)^2 \times [2.163 + 12.219\left(\frac{a_i}{W}\right) - 20.065\left(\frac{a_i}{W}\right)^2 - 0.9925\left(\frac{a_i}{W}\right)^3 + 20.609\left(\frac{a_i}{W}\right)^4 - 9.9314\left(\frac{a_i}{W}\right)^5] \quad (7a)$$

$$C_{LLi} = \frac{1}{EB_e}\left(\frac{S}{W-a_i}\right)^2 \times [1.193 - 1.98\left(\frac{a_i}{W}\right) + 4.478\left(\frac{a_i}{W}\right)^2 - 4.443\left(\frac{a_i}{W}\right)^3 + 1.739\left(\frac{a_i}{W}\right)^4] \quad (7b)$$

$$C_{LLi} = \frac{1}{EB_e}\left(\frac{W+a_i}{W-a_i}\right)^2 \times [2.0462 + 9.6496\left(\frac{a_i}{W}\right) - 13.7346\left(\frac{a_i}{W}\right)^2 + 6.1748\left(\frac{a_i}{W}\right)^3] \quad (7c)$$

where the effective thickness $B_e = B-(B-B_N)^2/B$.

Based on the crack size calculation in Eq. 1 and the corresponding J-integral calculation in Eq. 3, one example of the original DCPD J-R curve for a 0.18T DC(T) specimen made from MatA is shown in Fig. 4. The initial portion of the J-R curve in Fig. 4 indicates fast crack growth and does not follow the construction line closely, resulting in a relatively low J_q value. Indeed, as noted in the work of Bakker [21], the material potential drop can also result from deformation, crack blunting, and void growth in the process zone ahead of the crack during J-R curve tests. If the influences of these factors are not accounted for in the crack length prediction, the DCPD technique would not predict the crack size accurately and can result in much lower J_q values. Therefore, adjustment on the original DCPD J-R curve is needed. In early DCPD adjustment methods [22], a slope change point, counted as the critical point distinguishing crack blunting from the onset of slow stable crack growth, is identified by visual inspection of the displacement-potential drop curve. However, the slope change point in a displacement-potential drop curve may not be clearly identified on occasion and the selection of the critical point tends to be arbitrary, resulting in poor repeatability of the analysis. In a more recent work by Chen et al. [23], new DCPD adjustment methods were developed with improved repeatability and excellent match with the EUC and normalization methods in terms of J_q values. The major drawback in

that method is that the post-adjustment DCPD tearing modulus results show an average difference of 17% from the EUC and normalization results. A possible explanation for that result is that, since the potential gage span in that work was relatively large, the potential drop signal was measured from a large volume of material which enhanced the influence of plastic deformation on the DCPD measurement.

In order to address these issues, the distance between two potential probes was reduced as much as possible but still wide enough to cover the starter notch of a specimen and did not interfer with any displacement measurement devices. In addition, a newly-developed semi-empirical DCPD adjustment procedure is proposed. The DCPD adjustment procedure is mainly composed of two steps. The first step aims for identifying the critical point distinguishing crack blunting from the onset of slow stable crack growth. To achieve this, the first order derivative of the original DCPD J-R curve coupled with Savitzky-Golay [24] second order polynomial smoothing with 19 points of window is applied as shown in Fig. 5(a). The peak point in Fig. 5(a) represents the data point from which the slope of the original DCPD J-R curve starts to decrease and is indicative of the onset of slow stable crack growth. Therefore, the peak point is selected as the critical point. The combination of first order derivative of the original DCPD J-R curve and Savitzky-Golay smoothing eliminates the ambiguity in the selection of the critical point and greatly suppress the noise, if there is any, in the original DCPD J-R curve data for the critical point selection. Once the critical point is identified, all data points prior to and including the critical point itself from the original DCPD J-R curve are shifted left onto the construction line since these data points correspond to the plastic deformation and crack blunting stage of the specimen (Fig. 5(b)).

After crack initiation, stable crack growth dominates the increase in the potential drop although material deformation and specimen shape change may still influence the potential drop measurement. To address the influence of those factors on DCPD-predicted crack length at the stable crack growth stage, the second step of the DCPD adjustment procedure covers data points between the crack initiation point and the last point in a J-R curve. The concept of the second step adjustment is to force the final crack length prediction from the DCPD technique to match the optically measured final crack extension so that the final crack length prediction from the DCPD technique is correct. Assuming the crack size at crack initiation is correct after the first step adjustment in the DCPD technique, data points between the crack initiation point and final crack length measurement in a post-adjustment DCPD J-R curve should be reasonably valid. To realize this concept, crack sizes for data points subsequent to the critical point in the original DCPD J-R curve are adjusted such that the final crack extension prediction from the DCPD technique matches the measured final crack extension (Fig. 5(b)). To do so, the crack size of the i-th data point subsequent to the critical point in the original DCPD J-R curve is adjusted according to the following equation [21]:

$$a_{pdi'} = \Delta a_{pdcritical'} + \Delta a_{pdi} - \Delta a_{pdcritical} - \frac{u_{pdi} - u_{pdcritical}}{u_{pdfinal} - u_{pdcritical}} (\Delta a_{pdfinal} - \Delta a_{pdcritical} - \Delta a') \quad (8)$$

where $\Delta a_{pdcritical'}$ is the crack extension of the critical point after the first step adjustment, Δa_{pdi} is the original DCPD crack extension for the i-th data point, $\Delta a_{pdcritical}$ is the original crack extension of the critical point, u_{pdi} is the displacement value for the i-th data point, $u_{pdcritical}$ is the displacement value for the critical point, $u_{pdfinal}$ is the displacement value for the last data point in the J-R curve, $\Delta a_{pdfinal}$ is the original DCPD crack extension for the last data point in the J-R curve, and $\Delta a'$ is defined by:

$$\Delta a' = \Delta a_{measured} - \Delta a_{pdcritical'} \quad (9)$$

where $\Delta a_{measured}$ is the optically measured final crack extension.

Once the updated crack sizes from the two-step DCPD adjustment procedure become available, they are used to recalculate J-integral values since J-integral also depends on the crack size. Combining the recalculated J-integral and updated crack sizes forms the final DCPD J-R curve. One example for comparing the original DCPD J-R curve, the post-adjustment DCPD J-R curve, and the J-R curve from the normalization method is shown in Fig. 6. After adjustment, the DCPD J-R curve follows the construction line initially resulting in a much more reasonable J_q value compared with original DCPD J-R curve. In addition, the post-adjustment DCPD J-R curve is almost identical with the J-R curve from the normalization method.

Comparison of J-R Curves Determined by the Normalization Method and the DCPD Technique after Adjustment

The comparison of major J-R curve test results, namely J_q value and the J-R curve slope between two exclusions lines, are shown in Fig. 7. Excellent agreement is observed between J-R curves from the normalization method and post-adjustment DCPD J-R curves in most tests. The average differences for J_q and J-R curve slopes between the normalization method and the DCPD technique after adjustment are only 5.2% and 7.4%, respectively. Considering the variety of materials, specimen configurations, and testing temperatures investigated in this study, the DCPD technique and the newly-developed DCPD adjustment procedure show very promising results in the J-R curve characterization.

Conclusions

J-R curve testing was performed on a wide range of materials, specimen configurations, and testing temperatures to evaluate the applicability of the DCPD technique in the J-R curve

characterization. Results are compared with baseline J-R curves derived from the ASTM normalization method. The original J-R curves from the DCPD technique yielded much smaller J_q values than the normalization method due to the influence of crack blunting, plastic deformation, etc. on potential drop. To counter these effects, a new procedure for adjusting DCPD J-R curves was proposed. After applying the new adjustment procedure, the average difference in J_q between the DCPD technique and the normalization method was only 5.2% and the difference in tearing modulus was 7.4%. The promising result demonstrate the applicability of the DCPD technique for the J-R curve characterization especially in extreme environments, such as elevated temperatures, where the conventional EUC method faces considerable challenges.

Acknowledgement

The authors express appreciation to Richard Wright of Idaho National Laboratory and Sam Sham of Oak Ridge National Laboratory for programmatic support. This research was sponsored by the U.S. Department of Energy, Office of Nuclear Energy, Generation IV Reactor Research Program, under contract DE-AC05-00OR22725 with UT-Battelle, LLC. The authors also would like to extend their appreciation to Eric Manneschmidt for performing part of mechanical testing, and to Gene Ice, Thak Sang Byun, and Lauren Garrison for their technical reviews.

References

1. Zhu, X.K. Lam, P.S. and Chao, Y.J., "Application of Normalization Method to Fracture Resistance Testing for Storage Tank A285 Carbon Steel," *Int. J. Pres. Ves. Pip.*, Vol. 86, 2009, pp. 669-676.

2. ASTM E1820-13: Standard Test Method for Measurement of Fracture Toughness, *Annual Book of ASTM Standards,* ASTM International, West Conshohocken, PA, 2013.

3. Chen, X. Nanstad, R.K. and Sokolov, M.A., "J-R Curve Determination for Disk-Shaped Compact Specimens Based on the Normalization Method and the Direct Current Potential Drop Technique," *Sixth International Symposium on Small Specimen Test Techniques, ASTM STP 1576,* M. Sokolov and E. Lucon, Eds., ASTM International, West Conshohocken, PA, 2014, p. 1.

4. Herrera, R. and Landes, J.D., "Direct J-R Curve Analysis: A Guide to the Methodology," *Fracture Mechanics: Twenty-First Symposium, ASTM STP 1074*, J. Gudas, J. Joyce, and E. Hackett, Eds., ASTM International, West Conshohocken, PA, 1990, p. 24.

5. Landes, J. Zhou, Z. Lee, K. and Herrera, R., "Normalization Method for Developing J-R Curves with the Lmn Function," *J. Test. Eval.*, Vol. 19, 1991, pp. 305-311.

6. Joyce, J., "Analysis of a High Rate Round Robin Based on Proposed Annexes to ASTM E 1820," *J. Test. Eval.*, Vol. 29, 2001, pp. 329-351.

7. Lee, K., "Elastic-Plastic Fracture Toughness Determination under Some Difficult Conditions," PhD Dissertation, University of Tennessee, Knoxville, 1995.

8. Hicks, M.A. and Pickard, A.C., "A Comparison of Theoretical and Experimental Methods of Calibrating the Electrical Potential Drop Technique for Crack Length Determination," *Int. J. Fract.,* Vol. 20, 1982, pp. 91-101.

9. Lowes, J.M. and Featnehough, G.D., "The Detection of Slow Crack Growth in Crack Opening Displacement Specimens using an Electrical Potential Method," *Eng. Fract. Mech.,* Vol. 3, 1971, pp. 103-104.

10. McGowan, J.J. and Nanstad, R.K., “Direct Comparison of Unloading Compliance and Potential Drop Techniques in J-integral Testing,” *SEM Fall Conference, Computer-Aided Testing and Modal Analysis*, Milwaukee, WI, Nov. 4-7, 1984.

11. Ritchie, R.O. and Bathe, K.J., "On the Calibration of the Electrical Potential Technique for Monitoring Crack Growth using Finite Element Methods," *Int. J. Fract.*, Vol. 15, 1979, pp. 47-55.

12. Tong, J., "Notes on Direct Current Potential Drop Calibration for Crack Growth in Compact Tension Specimens," *J. Test. Eval.*, Vol. 29, 2001, pp. 402-406.

13. Chen, X. Nanstad, R.K. Sokolov, M.A. and Manneschmidt, E.T., “Determining Ductile Fracture Toughness in Metals,” *Adv. Mater. Process.*, Vol. 172, 2014, pp. 19-23.

14. ASTM E1921-13: Standard Test Method for Determination of Reference Temperature, T_o, for Ferritic Steels in the Transition Range, *Annual Book of ASTM Standards*, ASTM International, West Conshohocken, PA, 2013.

15. Landes, J. D., “J Calculation from Front Face Displacement Measurements of a Compact Specimen,” *Int. J. Fract.*, Vol. 16, 1980, pp. R183-186.

16. ASTM E647-11, Standard Test Method for Measurement of Fatigue Crack Growth Rates, *Annual Book of ASTM Standards*, ASTM International, West Conshohocken, PA, 2011.

17. Johnson, H.H., “Calibrating the Electrical Potential Method for Studying Slow Crack Growth,” *Mater. Res. Stand.*, Vol. 5, 1965, pp. 442-445.

18. Schwalbe, K.H. and Hellmann, D., "Application of the Electrical Potential Method to Crack Length Measurements using Johnson Formula," *J. Test. Eval.*, Vol. 9, 1981, pp. 218-220.

19. Turner, C.E., “The Eta Factor,” *Post Yield Fracture Mechanics, Second Ed.*, Elsevier Applied Science Publishers, London and New York, 1984, p. 451.

20. Chattopadhyay, J. Dutta, B.K. and Kushwaha, H.S., "New 'η_{pl}' and 'γ' functions to evaluate J–R curve from cracked pipes and elbows. Part I: theoretical derivation," *Eng. Fract. Mech.,* Vol. 71, 2004, pp. 2635-2660.

21. Bakker, A.D., "A DC Potential Drop Procedure for Crack Initiation and R-Curve Measurements During Ductile Fracture Tests," *Elastic-Plastic Fracture Test Methods: The User's Experience, ASTM STP 856,* F. Loss, and E. Wessel, Eds., ASTM International, West Conshohocken, PA, 1985, p. 394.

22. Dufresne, J. Henry, B. and Larsson, H., "Fracture Toughness of Irradiated AISI 304 and 316L Stainless Steels," *Effects of Radiation on Structural Materials, ASTM STP 683,* J. Sprague, and D. Kramer, Eds., ASTM International, West Conshohocken, PA, 1979, p. 511.

23. Chen, X. Nanstad, R.K. and Sokolov, M.A., "Application of Direct Current Potential Drop for Fracture Toughness Measurement," *22nd International Conference on Structural Mechanics in Reactor Technology,* San Francisco, CA, Aug. 18-23, 2013.

24. Savitzky, A. and Golay, M., "Smoothing + Differentiation of Data by Simplified Least Squares Procedures," *Anal. Chem.,* Vol. 36, 1964, pp. 1627-1639.

Tables

Table 1 Test matrix in J-R curve testing

Material	Specimen type	Temperature (°C)
Type 316LN stainless steel (MatA)	0.18T C(T)	24, 500
Ni-based alloy 617 (MatB)	0.5T C(T)	24, 250, 500, 650
Ferritic-martensitic steel (MatC)	0.5T C(T), 5x10 mm & 10x10 mm SE(B)	24, 114, 300, 500, 600

List of Figure Captions

Fig. 1 Issues in elevated temperature J-R curve testing using the EUC method: (a) material stress relaxation resulting in nonlinear unloading-reloading curves; (b) a back-up shape of the J-R curve induced by friction interference between the specimen and loading devices

Fig. 2 The crack length measurement principle in the DCPD technique

Fig. 3 Specimen configurations for (a) C(T), (b) SE(B), and (c) DC(T). The red arrows indicate the current probe locations and the green dot lines indicate the potential probe locations

Fig. 4 The original DCPD J-R curve of a 0.18T DC(T) specimen made from MatA

Fig. 5 (a) critical point selection based on the peak point of the first order derivative of the original DCPD J-R curve with Savitzky-Golay smoothing; (b) the two-step adjustment of the original DCPD J-R curve

Fig. 6 Comparison of the original DCPD J-R curve, the post-adjustment DCPD J-R curve, and the normalization-method J-R curve of a 0.18T DC(T) specimen made from MatA

Fig. 7 Comparison of J_q and dJ/da derived from the normalization J-R curves and post-adjustment DCPD J-R curves

Figures

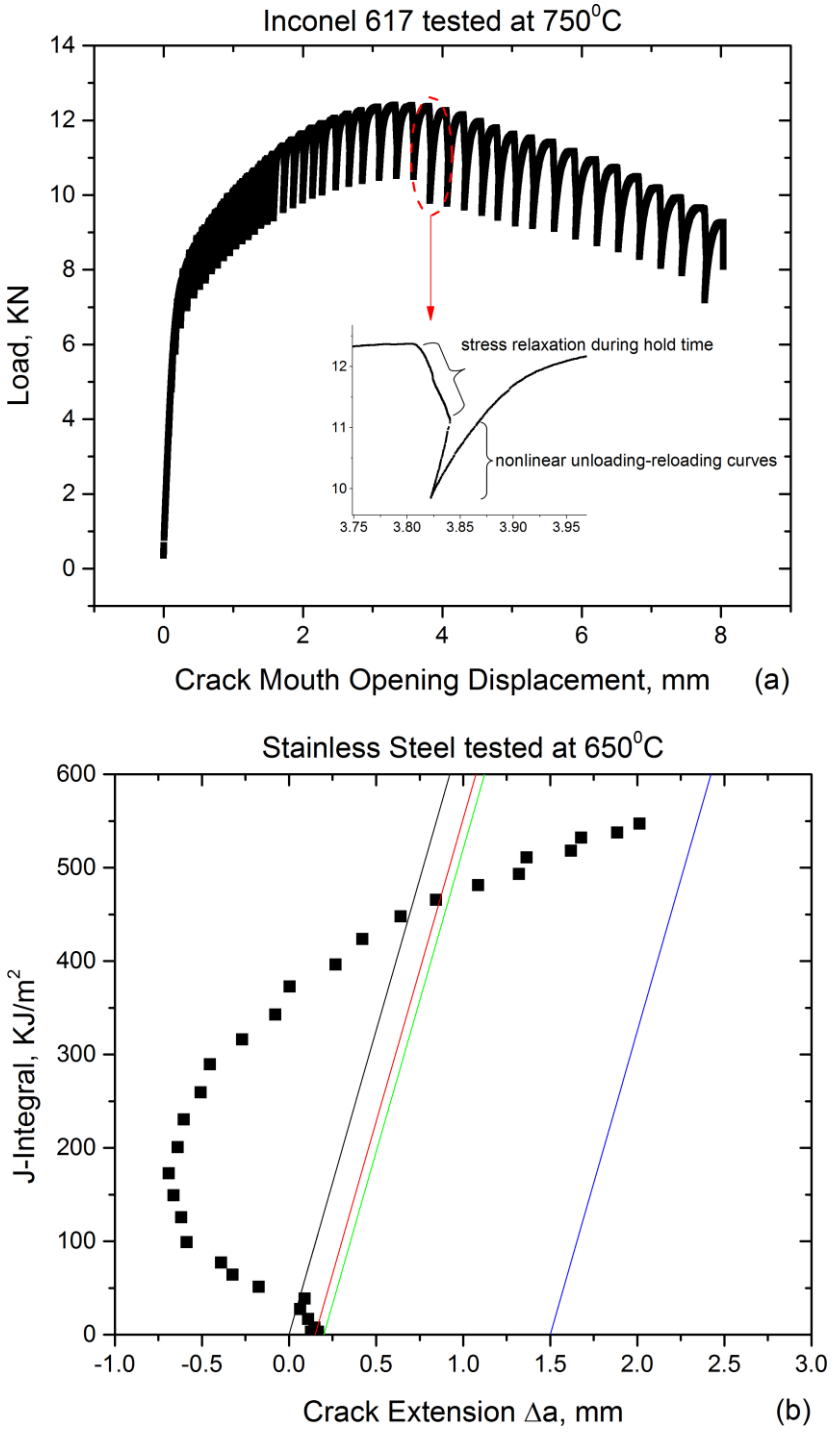

Fig. 1 Issues in elevated temperature J-R curve testing using the EUC method: (a) material stress relaxation resulting in nonlinear unloading-reloading curves; (b) a back-up shape of the J-R curve induced by friction interference between the specimen and loading devices

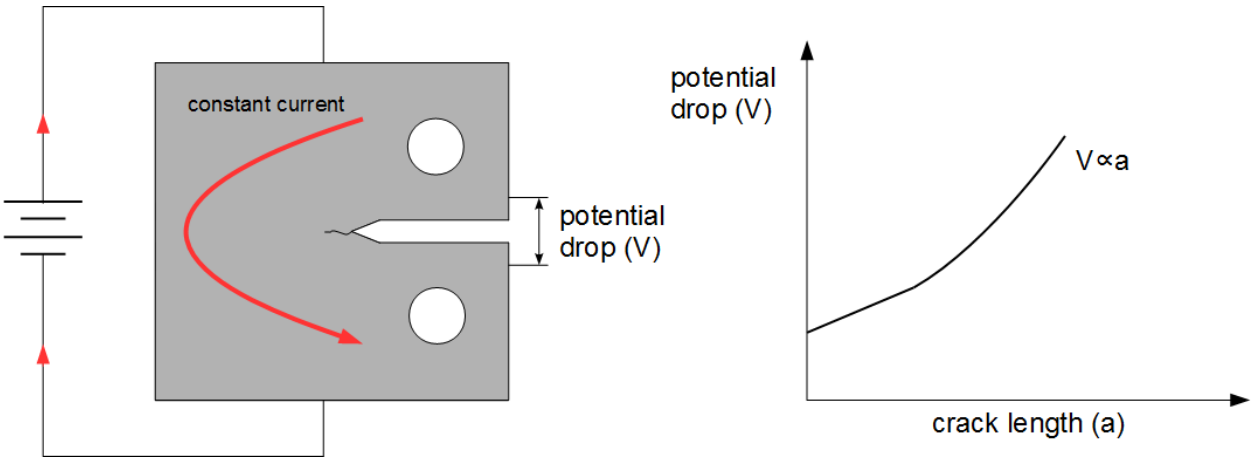

Fig. 2 The crack length measurement principle in the DCPD technique

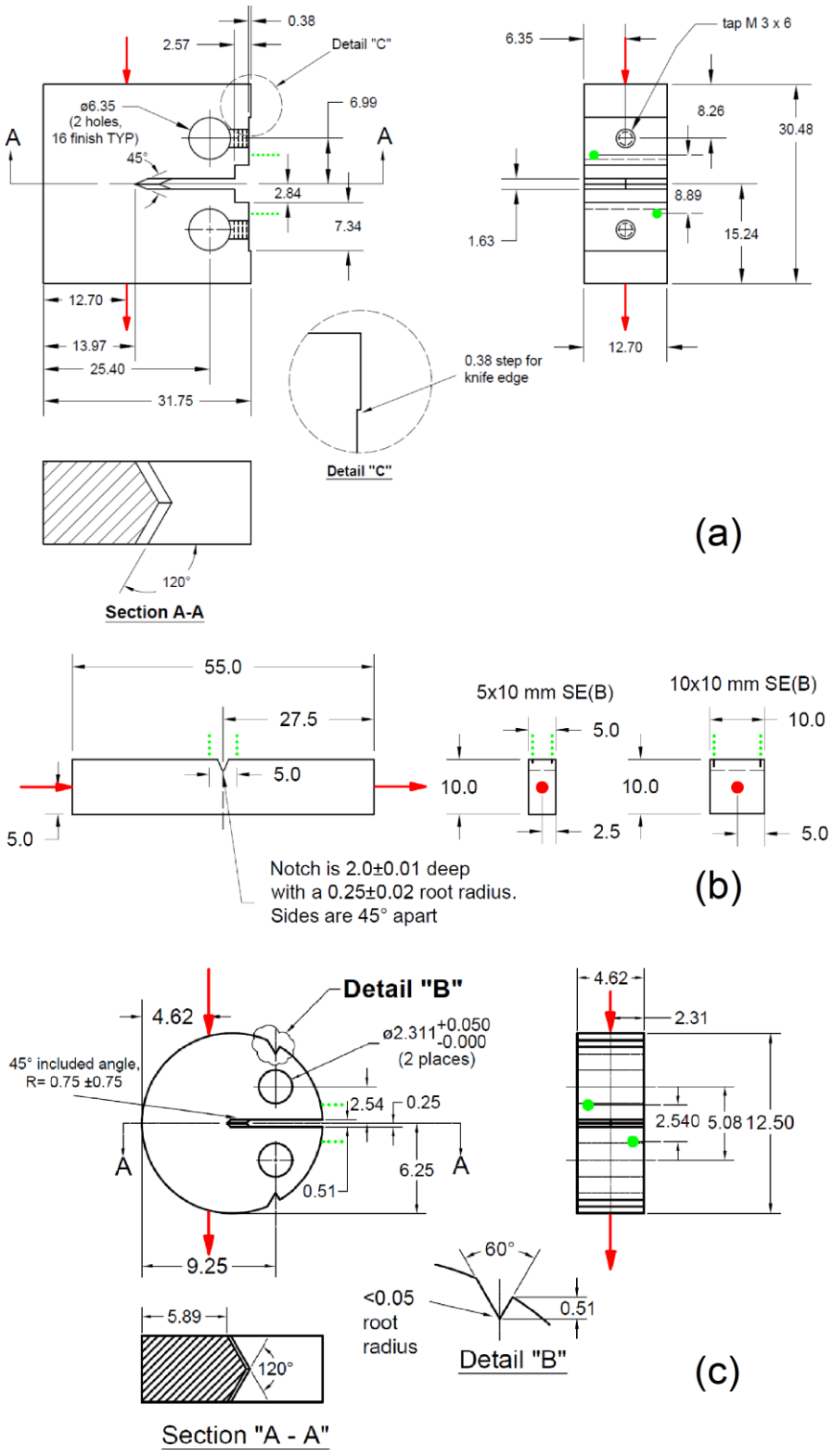

Fig. 3 Specimen configurations for (a) C(T), (b) SE(B), and (c) DC(T). The red arrows indicate the current probe locations and the green dot lines indicate the potential probe locations

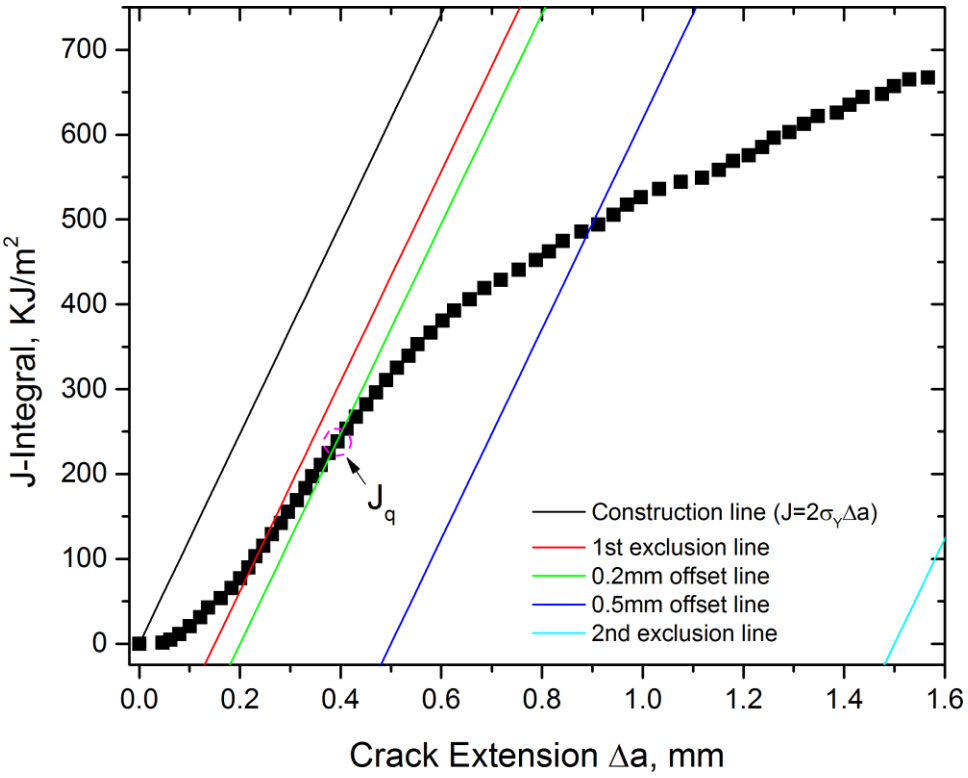

Fig. 4 The original DCPD J-R curve of a 0.18T DC(T) specimen made from MatA

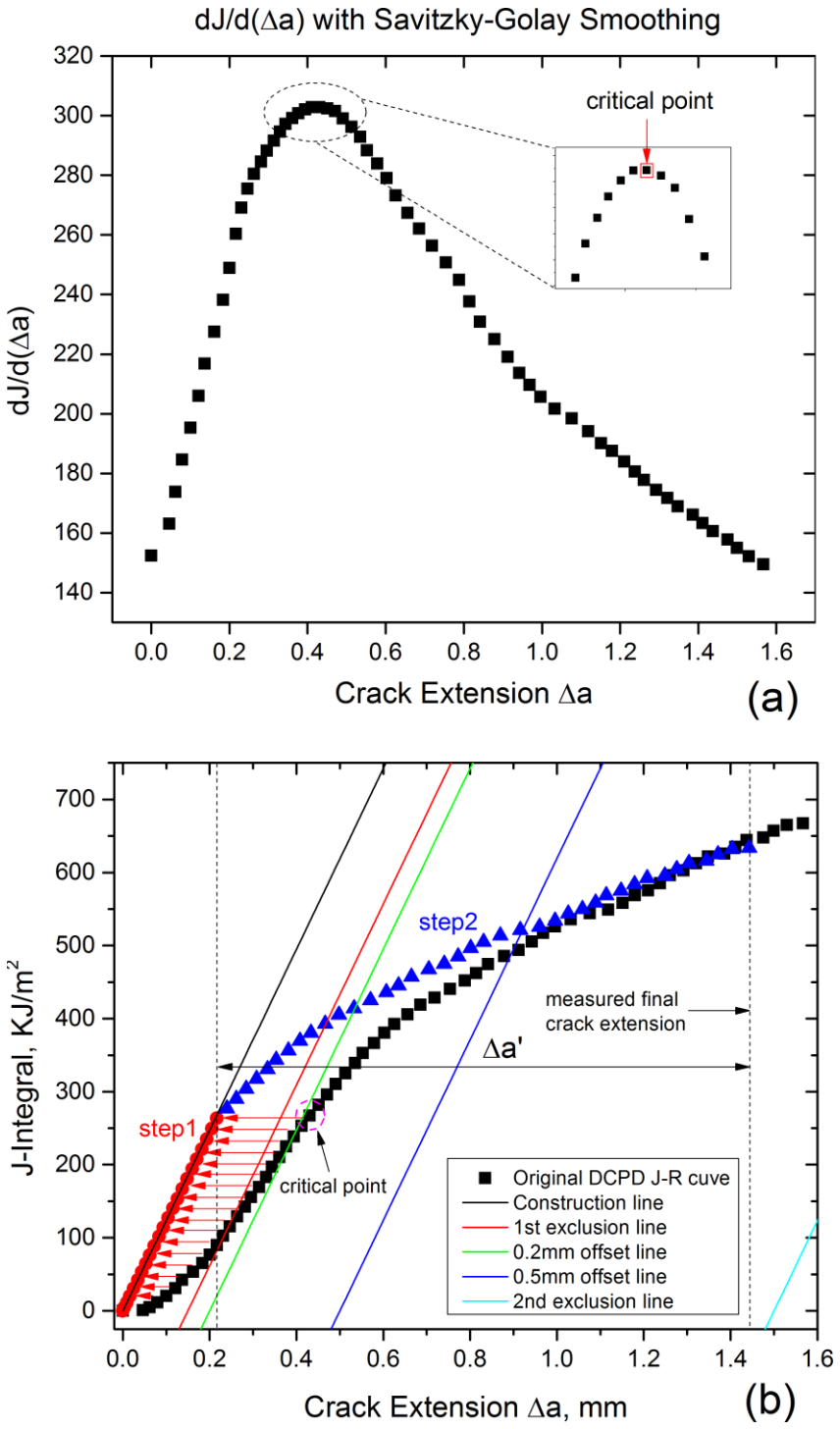

Fig. 5 (a) critical point selection based on the peak point of the first order derivative of the original DCPD J-R curve with Savitzky-Golay smoothing; (b) the two-step adjustment of the original DCPD J-R curve

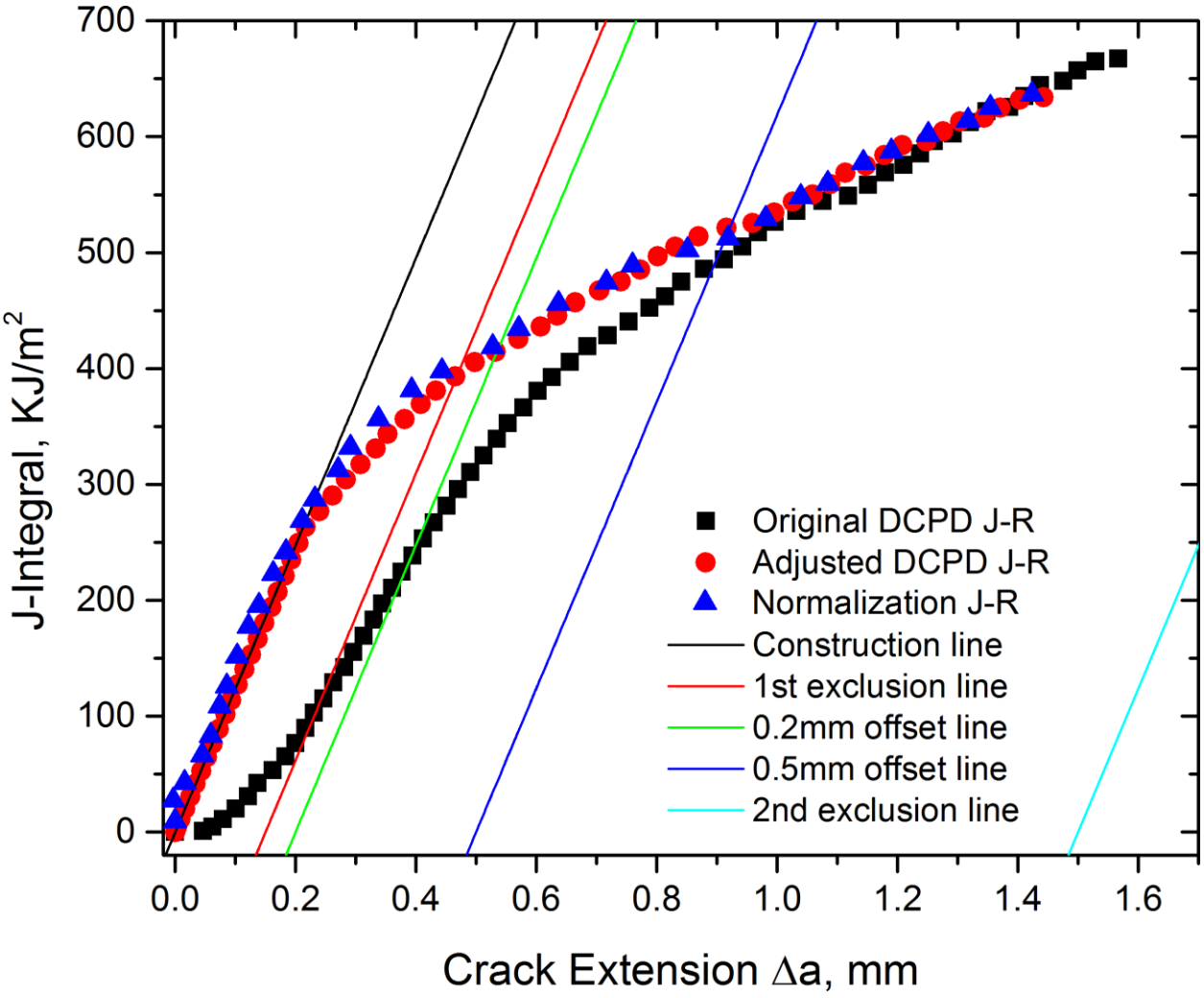

Fig. 6 Comparison of the original DCPD J-R curve, the post-adjustment DCPD J-R curve, and the normalization-method J-R curve of a 0.18T DC(T) specimen made from MatA

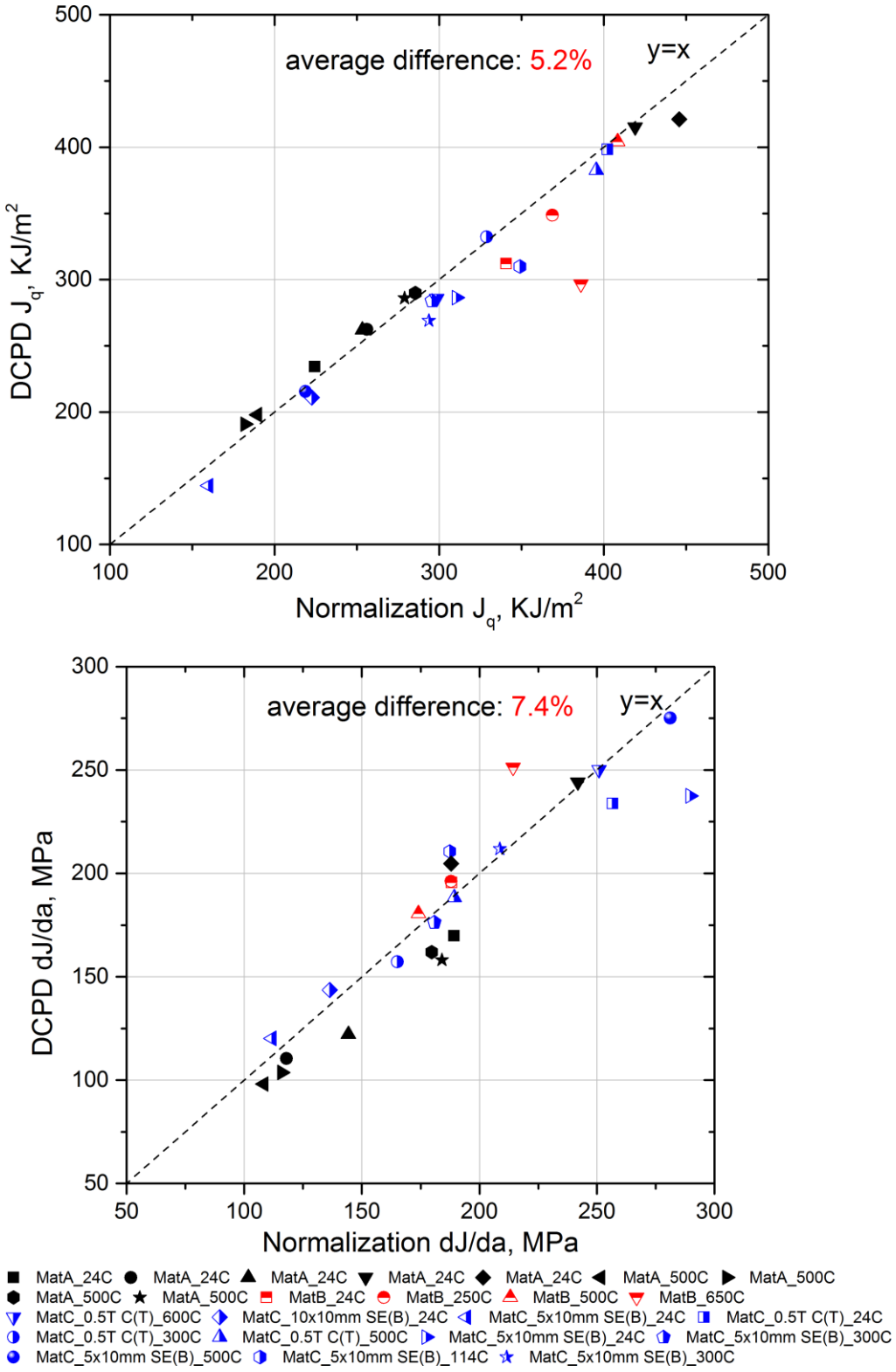

Fig. 7 Comparison of J_q and dJ/da derived from the normalization J-R curves and post-adjustment DCPD J-R curves